Structure of the Amorphous Phase in Crystallizable Polymers: Poly(ethylene terephthalate)

N. S. Murthy,* S. T. Correale, and H. Minor

Research and Technology, Allied-Signal, Inc., Morristown, New Jersey 07962

Received June 11, 1990; Revised Manuscript Received August 29, 1990

ABSTRACT: Evidence for spatial correlations of the polymer chains in the amorphous phase of crystallizable polymers is presented by using the X-ray diffraction patterns of poly(ethylene terephthalate) resins, films, and fibers. The necessity of resolving the amorphous halo between 5° and 35° 2θ (Cu Kα) into at least two peaks (s = 0.20 and 0.26 Å^{-1}) suggests that there can be more than one average interchain distance in the amorphous phase. The two distances might arise from the rotational correlations of the aromatic groups on adjacent chains. The relative intensity of the two amorphous peaks was found to depend on the thickness in quich-quenched films, on the temperature in variable-temperature scans of crystalline powders, and on the azimuthal angle in oriented fibers. These variations in the intensities of the two peaks are attributed to changes in the short-range ordering of the amorphous chain segments. Further, the nonzero base line in the plot of the variations in the scattered intensity with azimuthal angle suggests that the amorphous scattering can be conceptually separated into isotropic and anisotropic components.

Introduction

X-ray diffraction (XRD) studies of crystallizable polymers have typically emphasized the usefulness of XRD in determining and following the changes in crystalline structures and in the routine determination of the crystallinity levels. Even though the diffuse scattered intensity from the amorphous regions contains information about the structural order in the amorphous domains, the amorphous background is usually regarded as a nuisance that one has to deal with in evaluating the integrated intensities of the crystalline peaks. In a recent paper, we proposed how the contribution of the amorphous phase can be derived from the XRD scans of crystallizable polymers by stripping the easily identifiable crystalline features.[1] The resulting amorphous scattering profile was then used as a template in evaluating crystallinity, especially in samples with low crystalline content. We noted that in many instances the amorphous halo, even within an angular range of 2θ = 15–30° (Cu Kα), had to be described by more than one peak. In that paper we refrained from offering any interpretations for our observations. We will now suggest that the different peaks in the amorphous phase represent order along different crystallographic directions. We also present evidence for incipient crystalline order in samples that would be normally classified as amorphous by XRD.

Materials and Methods

A low molecular weight (M_w = 3000, IV = 0.08 dL/g) poly(ethylene terephthalate) (PET) powder was studied as an example of a highly crystalline sample. A crystalline and two amorphous films were prepared from a PET resin of IV = 0.53 dL/g. An amorphous PET plaque prepared from a resin with an IV = 0.7 dL/g was also included in the series. PET resins (IV = 0.95 dL/g) were molded into films of thicknesses ranging from 0.05 to 1.7 mm. This PET resin was used for variable-temperature measurements. Oriented yarns were made with PET with an IV = 0.90 dL/g.

XRD scans from powders, films, and plaques were obtained in the parafocus mode on a Philips diffractometer. XRD scans from amorphous, oriented PET yarns were obtained on a Philips diffractometer in the transmission mode. Several radial scans were made at various azimuthal angles (ϕ). XRD data from PET powder at various temperatures were obtained by using an Anton-Paar variable-temperature attachment. The data were collected from powdered PET, sprinkled as a thin layer on a copper block whose temperature was electronically controlled. A thin layer of sample was needed to avoid any thermal gradients.

The diffraction scans were analyzed by using a modified version of the program "SHADOW".[1,2] The peak shapes for the scans obtained in the parafocus geometry were modeled by a modified Lorentzian function, $I(x) = I(0)/(1 + kx^2)$, $k = 0.4142\,(\text{fwhm}/2)^{-2}$, $x = 2\theta - 2\theta_k$, in which $I(x)$ is the scattered intensity at x, x is the distance from the Bragg angle $2\theta_k$ for the reflection, 2θ is the scattering angle, and fwhm is the full-width at half-maximum of the reflection (peak). It has been found from the analysis of crystalline peaks from polycrystalline inorganic powders that the modified Lorentzian functions provide the best fit to the reflections in the parafocus geometry. The peak parameters were generally not constrained during the profile analysis, except for the high-temperature (200, 240, and 290 °C) scans in which the positions of the amorphous peaks were limited to a small range about the corresponding positions in the amorphous template obtained from analyzing the highly crystalline sample.[1]

Gaussian functions were found to adequately describe the diffraction peaks in the transmission geometry. The radial scans from oriented amorphous PET fibers were resolved into two amorphous peaks. The positions of the amorphous peaks were allowed to vary over a small range about the value determined from a template.

Results

Figure 1a shows the XRD pattern from a highly crystalline sample of "oligomeric" (M_w = 3000) PET powder resolved into crystalline peaks. The intensity not attributable to these crystalline peaks is assumed to be due to the noncrystalline or the amorphous phase. We were unable to fit the diffuse scattered intensity from the amorphous phase (the amorphous halo) to one peak. At least two peaks (2θ = 17.5°, s = 0.20 Å^{-1} and 2θ = 23.5°, s = 0.26 Å^{-1}; $s = (2 \sin\theta)/\lambda$) were always necessary to fit the scattering even from the most "amorphous" sample. XRD data from a typical PET sample (an annealed film) are shown in Figure 1b resolved into amorphous and crystalline peaks. Note the difference in the relative heights of the two amorphous halos in the oligomer and the typical polymeric sample. The XRD scans from PET films of various thicknesses quick-quenched from the melt were resolved into amorphous peaks as shown in Figure 2. The relative intensities of the two amorphous peaks vary with the thickness of the films. The ratios of the areas of the two components of the amorphous halo for the various films are listed in Table I.

Radial XRD scans from oriented, amorphous PET yarns at a series of azimuthal angles (ϕ) are shown in Figure 3.

0024-9297/91/2224-1185$02.50/0

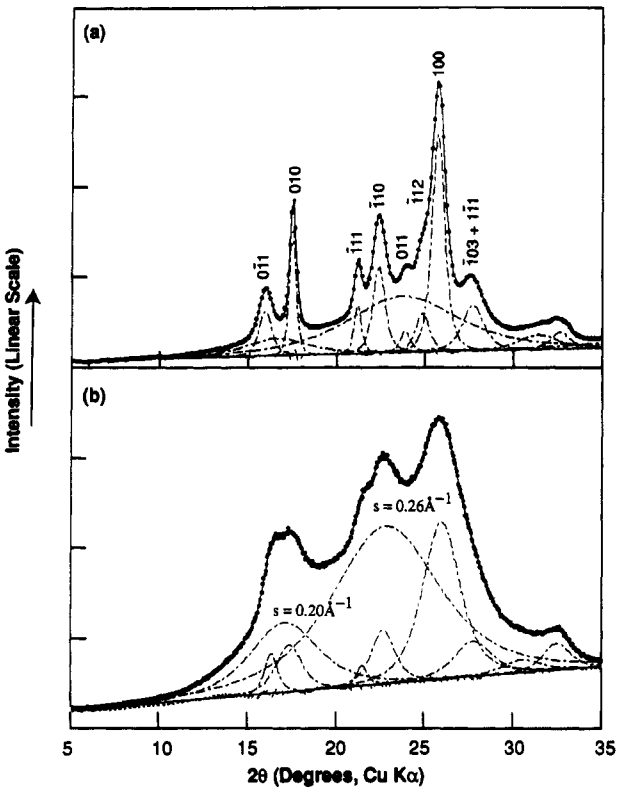

Figure 1. Profile-fitted XRD scans of various PET samples. (a) Highly crystalline powder from low molecular weight (IV = 0.08) PET. (b) Scan of a typical annealed film. In this and the following profile-fitted scans, the full line that overlaps the observed data (points) represents the sum of the resolved components (dashed lines). The dashed line over the base line (full line) is the difference between the observed intensities and the calculated curve.

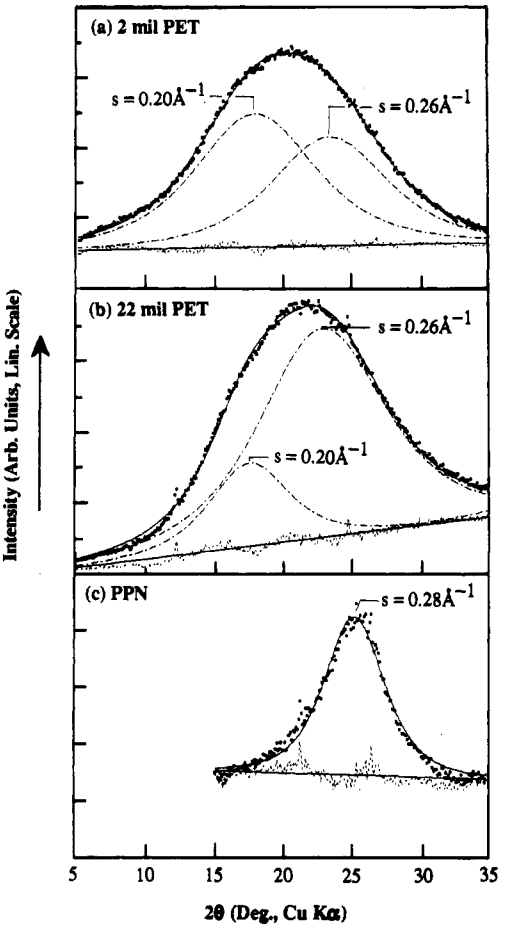

Figure 2. Profile-fitted XRD scans of PET films of thickness of (a) 0.05 mm and (b) 0.56 mm. The scans from films or plaques thicker than 0.56 mm are similar to the curve in b (see Table I). (c) Profile-fitted scan of PPN. The sharp peaks in the residue are due to the unreacted polycrystalline precursor.

The two resolved scans in Figure 4 show that two amorphous peaks are indeed essential to fit the data even in the small angular range of $2\theta = 5$–$35°$. The areas of the two amorphous halos are plotted as a function of the azimuthal angle in Figure 5. The 0.26-Å^{-1} peak is more intense than the 0.20-Å^{-1} peak, but the degree of orientation of the two peaks is essentially the same within the sensitivity of our measurements. Unlike the off-equatorial scans, the scans close to the equator in our data could be resolved into a pair of amorphous peaks with a range of heights and half-widths. Hence, the errors in the peak intensities of the two amorphous halos near the equator ($\phi < 20°$) may be somewhat larger than at higher azimuthal angles.

XRD scans obtained from a PET powder at various temperatures are shown in Figure 6 resolved into amorphous and crystalline peaks. The results of the profile analysis are given in Table I. Crystalline peaks can be resolved in the 22, 190, and 200 °C scans, and these crystalline features disappear at 240 °C, which is close to the melting point of PET. The amorphous halo is asymmetric at 240 °C and becomes more symmetric at 290 °C. The implications of this asymmetry in understanding the packing of the PET chains (structure) in the amorphous regions will be discussed later.

The errors in the areas of the amorphous peaks obtained from profile analysis can be large. From repeated fits of the data with various starting parameters and constraints, we estimate the error (the difference between the maximum and minimum values) in our area ratios listed in Table I is typically ca. 10%, but, in some rare instances, can be as high as 50%. Data with much better counting statistics are necessary to reduce these errors. The results of peak resolution for scans in which the crystalline peaks are present (Figures 1a,b and 6a,b) show that the relative intensities of the crystalline peaks are about the same, suggesting that the profile analysis is satisfactory. In all the other scans, there was no evidence for the presence of crystalline peaks; this was confirmed by the calculation of second derivatives by Fourier analysis of the data with good counting statistics (ca 50 000 counts near the peak) from amorphous PET samples.

Discussion

According to Flory, conformations of polymer chains in the amorphous state correspond very closely to those of unperturbed random coils.[3] The agreement between the radius of gyration, R_g, of deuterium-labeled chains in the solid phase and that in a Θ-solvent is consistent with these predictions. However, local orientational order, and in many cases even crystallization, does not significantly affect R_g.[4] Therefore, the spatial trajectories of the polymer chains in the amorphous domains in crystallizable polymers could be significantly different from those of an unperturbed chain, even if the R_g's are the same. Spectroscopic, thermal, electron microscopy, and XRD data have suggested that there may be some kind of order in the amorphous regions in PET.[5-7] For instance, while XRD scans suggested that PET was amorphous, a consistently measurable amount of order was observed by IR:[7] the percent of trans $-OCH_2CH_2O-$ conformation, the conformation of the chains in the crystalline phase, was significantly higher than the 7% found in the amorphous

Table I
Ratios of the Two Amorphous Peaks between 2θ of 5–35° in Various PET Samples

sample	2θ values,[a] deg 0.20 Å^{-1}	2θ values,[a] deg 0.26 Å^{-1}	ratio of the areas 0.26 Å^{-1}/0.20 Å^{-1}	fwhm,[b] deg 0.20 Å^{-1}	fwhm,[b] deg 0.26 Å^{-1}
low mol wt powder	16.5	23.7	5.82	4.2	7.4
crystalline film	17.0	22.8	3.56	4.6	7.2
amorph film no. 1	18.1	23.3	2.51	6.5	9.3
no. 2	17.7	23.1	4.63	6.3	10.7
amorph plaque	17.4	22.9	4.60	6.7	11.1

thickness (mm) of the films	2θ values,[a] deg 0.20 Å^{-1}	2θ values,[a] deg 0.26 Å^{-1}	ratio of the areas 0.26 Å^{-1}/0.20 Å^{-1}	fwhm,[b] deg 0.20 Å^{-1}	fwhm,[b] deg 0.26 Å^{-1}
1.7	18.0	23.2	4.18	6.9	10.8
0.81	18.0	23.3	3.96	6.7	10.6
0.56	17.6	23.0	3.98	6.8	10.8
0.05	18.1	23.5	0.79	10.4	10.0

temp of the powder, °C	2θ values,[a] deg 0.20 Å^{-1}	2θ values,[a] deg 0.26 Å^{-1}	ratio of the areas 0.26 Å^{-1}/0.20 Å^{-1}	fwhm,[b] deg 0.20 Å^{-1}	fwhm,[b] deg 0.26 Å^{-1}
22	16.5	23.1	1.0	5.0	7.5
190	16.3	23.0	0.96	6.3	7.5
200	16.4	22.5	0.55	8.2	7.2
240	16.5	22.4	0.59	8.6	10.8
290	16.4	22.4	0.25	8.8	8.0

[a] $s = (2 \sin \theta)/\lambda$. [b] fwhm = full-width at half-maximum.

phase by Stokr et al.[8] Also, the density measurements showed that the samples, which were amorphous by XRD, had detectable levels of ordering in the amorphous phase.[7] Such discrepancies, as well as differences in the crystallinity calculated from various techniques (IR, XRD, NMR, thermal analysis, and density measurements), can be traced to the differences in the contributions of the structures in the amorphous phase to the various measurements. In this paper we will provide a means of analyzing the order in the amorphous regions by XRD. We will show that the multiple-peak model, which we introduced as an analytical convenience in our earlier paper,[1] could be of physical significance.

The plot of the intensities of the two peaks in oriented amorphous PET fibers as a function of the azimuthal angle ϕ shows that the two peaks reach a maximum at the equator (Figure 5). Therefore, the 0.20- and 0.26-Å peaks correspond to the two distances transverse to the chain axis. The two-peak model being discussed here for PET is also valid for other polymers in which the aromatic rings are parallel in the crystalline phase. In thermotropic liquid-crystalline polyesters, for instance, there are two peaks at 0.22 and 0.25 Å^{-1} according to Thomas and Wood[9] and at 0.22 and 0.26 Å^{-1} according to Mitchell and Windle.[10] These authors conclude that the two peaks are due to interchain interferences and represent biaxial packing of the adjacent chains. Our data show that such a packing need not be restricted to liquid-crystalline polyesters but could be present in PET as well. Such enhanced ordering in the amorphous phase might arise from rotational correlations of the aromatic groups on adjacent chains. Although we analyzed diffraction scans from $2\theta = 5$–35°, the analysis could be extended to include data from even higher angles. XRD data at higher angles have significant contributions from structures over distances of less than 4 Å, which include intramolecular interferences.[11] By considering data only at $2\theta < 35°$, we are restricting our discussion to

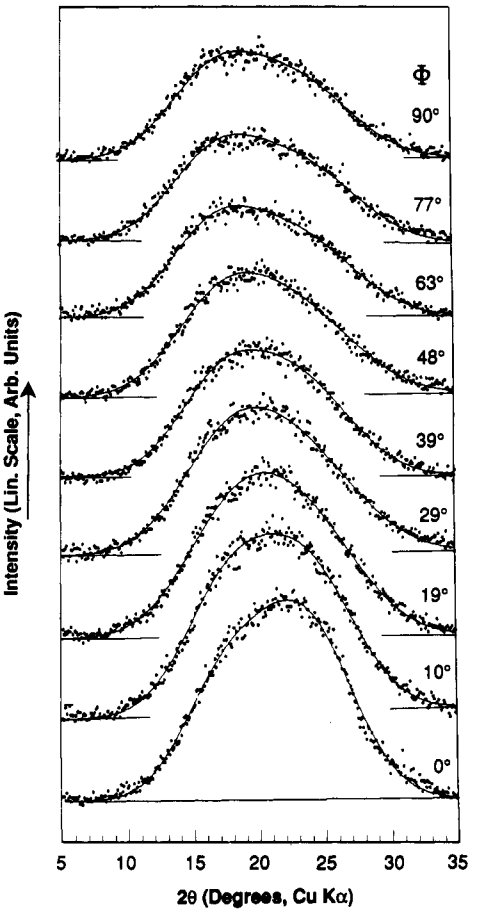

Figure 3. Radial XRD scans of the amorphous halo of an oriented, amorphous PET fiber at various azimuthal angles ϕ as indicated next to the curves. The full lines through the observed data points are the calculated profiles (see Figure 4).

intermolecular structures.

In the azimuthal scans of oriented, amorphous PET fibers (Figure 5), the intensity of the amorphous peaks does not become zero even at the meridian. We attribute this nonzero base line to the scattering from unoriented amorphous chain segments, while the oriented amorphous domains contribute to the scattered intensity to the peak above the base line. This suggests that the amorphous phase can be regarded as a two-component system, the oriented (anisotropic) and the unoriented (isotropic) components.[12–14] The amorphous chain segments represented by both of these components can be ordered.

The higher intensity of the 0.26-Å^{-1} peak along the equator in oriented fibers (Figure 5) suggests that the interchain distances corresponding to this peak are more prevalent in chains oriented parallel the fiber axis. The 0.26-Å^{-1} peak is also observed in the less ordered phases of carbon, and in these materials this peak is regarded as equivalent to a 002 basal reflection of graphite. For instance, in poly(*peri*-naphthalene) (obtained from low-temperature (530 °C) pyrolysis of perylenetetracarboxylic dianhydride), which is regarded as one-dimensional graphite, the 0.26-Å^{-1} peak (Figure 2c) can be attributed to the distance between the aligned aromatic groups on adjacent chains.[15] Further, in PET, the position of this amorphous peak is close to the intense 100 crystalline reflection (0.29 Å^{-1}; Figure 1). Thus, the 0.26-Å^{-1} peak corresponds to the interchain distances normal to the aligned aromatic rings (Figure 7). Similarly, since the 0.20-Å^{-1} peak occurs at the same 2θ value as the 010 reflection (0.20 Å^{-1}), we suggest that a fraction (see below) of the intensity in this amorphous peak is due to inter-

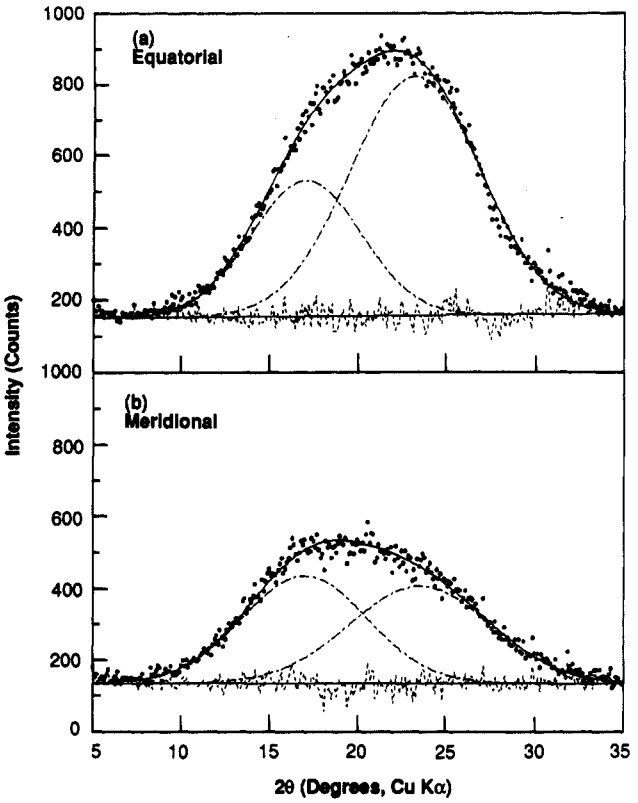

Figure 4. XRD scans of oriented, amorphous PET fibers resolved into two amorphous peaks. (a) Equatorial; (b) meridional.

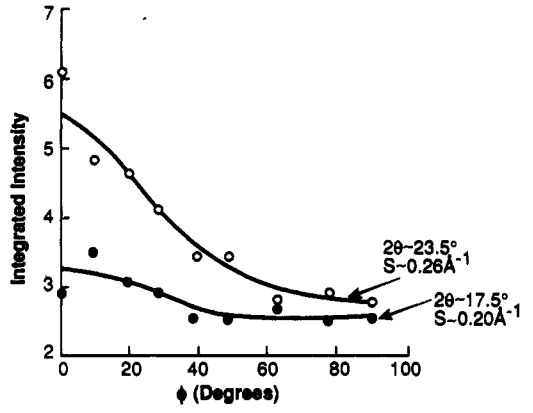

Figure 5. Azimuthal intensity variations of the two amorphous peaks in oriented amorphous PET fibers.

chain distances in the plane of the aromatic rings (Figure 7). The interpretation of the halo in terms of distances along two crystallographic directions suggests that incipient crystalline order can be present even in the amorphous phase.

Variable-temperature data show that the intensity of the 0.20-Å^{-1} peak relative to that of the 0.26-Å^{-1} peak increases with temperature (Figure 6). The 0.20-Å^{-1} peak is also intense in thin, quick-quenched films (Figure 2a). Hence, the 0.20-Å^{-1} peak, which corresponds to larger interchain distances, has a contribution from structures that may be equivalent to that present in the melt. Thus, while the 0.26-Å^{-1} peak is exclusively due to interchain distance normal to the aligned aromatic groups, the 0.20-Å^{-1} peak is probably a composite of distances in the plane of the aromatic groups between rotationally correlated chains and distances between chains that are randomly oriented around the chain axis. For instance, a higher intensity of the 0.20-Å^{-1} peak in the polymeric PET compared to that of oligomeric PET (Figure 1) might correspond to a higher

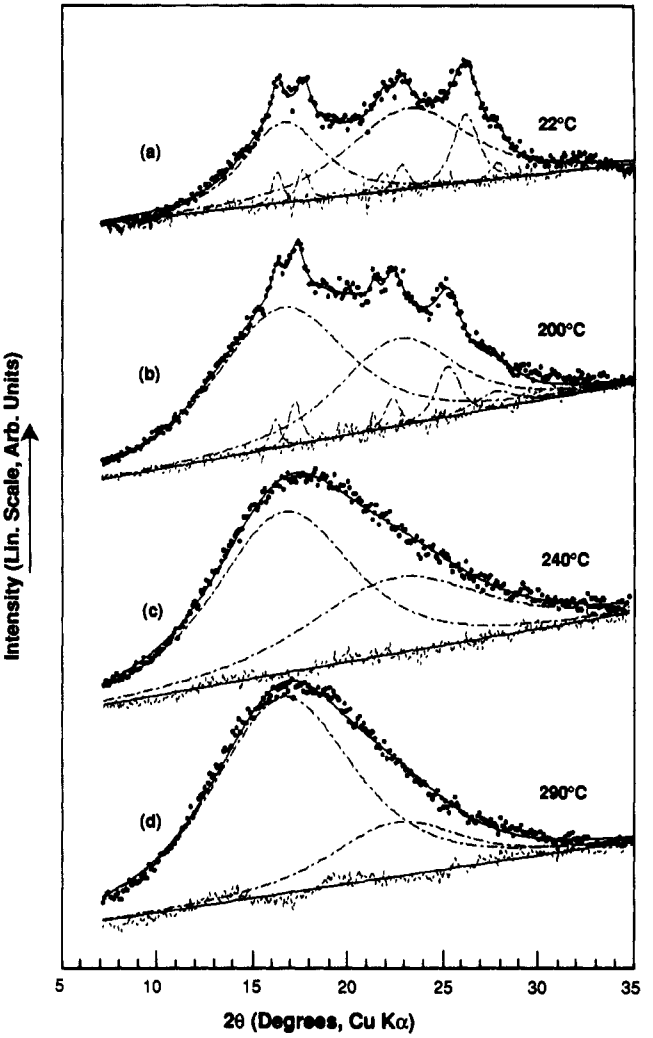

Figure 6. Variable-temperature scans from PET powder. Four typical scans are shown resolved into crystalline and amorphous peaks.

fraction of the disordered amorphous chain segments in the polymer as compared to the oligomer. Further, the variations in the position of the 0.20-Å^{-1} peak could be due to variations in the relative intensities of the two components. The 0.20-Å^{-1} peak might shift to higher angles as the orientation of the chains about the chain axis becomes more random. On the other hand, the shift in the position of the 0.26-Å^{-1} peak to lower angles with an increase in temperature (Table I) is probably due to thermal expansion.

The interpretation of the two peaks in the amorphous halo in terms of the structure in the amorphous regions becomes useful in analyzing the data from samples with low levels of crystallinity, such as quick-quenched PET films of various thicknesses (Figure 2). The extent of short-range, orientational correlations can be estimated from the relative heights of the various amorphous peaks, in our case of the two peaks between 5° and 35°. The heights of the two peaks are about the same in thin films, whereas the 0.26-Å^{-1} peak is more intense in thick films. Since the interior of a film cools slower than the skin, a thin film can be quenched more uniformly throughout its thickness than in a thick film. Therefore, the higher intensity of the 0.26-Å^{-1} peak can be regarded as evidence for enhanced molecular ordering in the interior of the thicker film. Thus, the order in the amorphous regions, as seen by the asymmetry of the amorphous halo, i.e., by the variations in the heights of the two amorphous peaks, depends upon

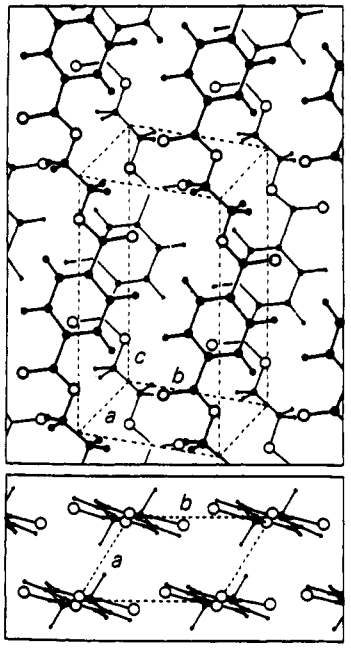

a = 4.56Å α = 98.5°
b = 5.94Å β = 118°
c = 10.75Å γ = 112°

2θ (010) = 17.5° 2θ (100) = 25.7°
s (010) = 0.20Å^{-1} s (100) = 0.29Å^{-1}

Figure 7. Crystal structure of PET (reproduced from ref 16 with permission of ICI Chemicals and Polymers Limited, Cleveland, U.K., and the Royal Society, London). Top, projection normal to 010 plane; bottom, projection along the c (chain) axis. Larger dots, carbon; smaller dots, hydrogen; open circles, oxygen.

the thermomechanical history of the samples. Further, the amorphous halo is asymmetric in the melt at T_m and becomes symmetric as the temperature is raised above T_m. This suggests that local order is present even in the melt, and the extent of this order decreases with an increase in the temperature of the melt. Such short-range order in the melt can give rise to longer relaxation times.

Conclusion

The presence of at least two average interchain distances (0.20 and 0.26 Å^{-1}) suggests that the amorphous phase in PET need not always be disordered. The 0.26-Å^{-1} peak is attributed to the interchain distances normal to the plane of the aligned aromatic rings; the 0.20-Å^{-1} peak is attributed to distances between the chains in the plane of these aromatic rings, as well from chains whose orientations around the chain axis are uncorrelated. The order in the amorphous phase can be evaluated by comparing areas of the two amorphous peaks. The amorphous phase in oriented samples can be resolved into oriented and unoriented components. The two-dimensional correlation transverse to the chain axis can be found in both the components but is expected to be higher in the oriented component.

Acknowledgment. We thank Dr. S. M. Aharoni and Prof. S. Krimm for valuable discussions and Dr. Z. Iqbal for his permission to include the data from PPN.

References and Notes

(1) Murthy, N. S.; Minor, H. *Polymer* **1990**, *31*, 996.
(2) Howard, S. A. *Adv. X-ray Anal.* **1989**, *32*, 523.
(3) Flory, P. J. *Principles of Polymer Chemistry*; Cornell University Press: Ithaca, NY, 1953; p 602.
(4) Wendorff, J. H. *Polymer* **1982**, *23*, 543.
(5) Fischer, E. W.; Fakirov, S. *J. Mater. Sci.* **1976**, *11*, 1041.
(6) Lee, S.; Miyaji, H.; Geil, P. H. *J. Macromol. Sci., Phys.* **1983**, *B22*, 489.
(7) Aharoni, S. M.; Sharma, R. K.; Szobota, J. S.; Vernick, D. A. *J. Appl. Polym. Sci.* **1983**, *28*, 2177.
(8) Stokr, J.; Schneider, B.; Doskocilova, D.; Lovy, J.; Sedlacek, P. *Polymer* **1982**, *23*, 714.
(9) Thomas, E. L.; Wood, B. A. *Faraday Discuss. Chem. Soc.* **1985**, *79*, 229.
(10) Mitchell, G. R.; Windle, A. H. *Polymer* **1982**, *23*, 1269.
(11) Wignall, G. D. *Applied Fibre Science*; Happey, F., Ed.; Academic Press: New York, 1975; Vol. 1, p 181.
(12) Harget, P. J.; Oswald, H. J. *J. Polym. Sci., Polym. Phys. Ed.* 1979, *17*, 531.
(13) Murthy, N. S.; Correale, S. T.; Moore, R. A. F. *J. Appl. Polym. Sci., Appl. Polym. Symp.* **1991**, *47*.
(14) Lindner, W. L. *Polymer* **1973**, *14*, 9.
(15) Iqbal, Z.; Ivory, D. M.; Marti, J.; Bredas, J. L.; Baughman, R. H. *Mol. Cryst. Liq. Cryst.* **1985**, *118*, 103.
(16) Daubeny, R. P.; Bunn, C. W.; Brown, C. J. *Proc. R. Soc., London* **1954**, *A226*, 531.

Registry No. PET, 25038-59-9.